Triple junction kinematics accounts for the 2016 M_w 7.8 Kaikoura earthquake rupture complexity

Xuhua Shi[a,b,1], Paul Tapponnier[c,1], Teng Wang[d], Shengji Wei[e], Yu Wang[f], Xin Wang[g], and Liqing Jiao[h]

[a]School of Earth Sciences, Zhejiang University, 310027 Hangzhou, China; [b]Research Center for Structures in Oil- and Gas-Bearing Basins, Ministry of Education, 310027 Hangzhou, China; [c]Key Laboratory of Crustal Dynamics, Institute of Crustal Dynamics, China Earthquake Administration, 100085 Beijing, China; [d]School of Earth and Space Sciences, Peking University, 100871 Beijing, China; [e]Earth Observatory of Singapore, Nanyang Technological University, Singapore 639798, Singapore; [f]Department of Geosciences, National Taiwan University, 10617 Taipei, Taiwan; [g]Seismological Laboratory, California Institute of Technology, Pasadena, CA 91125; and [h]Institut de Physique du Globe de Paris, Sorbonne Paris Cité, Université Paris Diderot, UMR 7154 CNRS, 75005 Paris, France

Contributed by Paul Tapponnier, November 6, 2019 (sent for review September 30, 2019; reviewed by Vincent Courtillot and Gilles Peltzer)

The 2016, moment magnitude (M_w) 7.8, Kaikoura earthquake generated the most complex surface ruptures ever observed. Although likely linked with kinematic changes in central New Zealand, the driving mechanisms of such complexity remain unclear. Here, we propose an interpretation accounting for the most puzzling aspects of the 2016 rupture. We examine the partitioning of plate motion and coseismic slip during the 2016 event in and around Kaikoura and the large-scale fault kinematics, volcanism, seismicity, and slab geometry in the broader Tonga–Kermadec region. We find that the plate motion partitioning near Kaikoura is comparable to the coseismic partitioning between strike-slip motion on the Kekerengu fault and subperpendicular thrusting along the offshore West–Hikurangi megathrust. Together with measured slip rates and paleoseismological results along the Hope, Kekerengu, and Wairarapa faults, this observation suggests that the West–Hikurangi thrust and Kekerengu faults bound the southernmost tip of the Tonga–Kermadec sliver plate. The narrow region, around Kaikoura, where the 3 fastest-slipping faults of New Zealand meet, thus hosts a fault–fault–trench (FFT) triple junction, which accounts for the particularly convoluted 2016 coseismic deformation. That triple junction appears to have migrated southward since the birth of the sliver plate (around 5 to 7 million years ago). This likely drove southward stepping of strike-slip shear within the Marlborough fault system and propagation of volcanism in the North Island. Hence, on a multimillennial time scale, the apparently distributed faulting across southern New Zealand may reflect classic plate-tectonic triple-junction migration rather than diffuse deformation of the continental lithosphere.

New Zealand | triple-junction migration | Kaikoura–Kermadec sliver plate | Kaikoura earthquake | rupture complexity

As long known and thoroughly studied, the twin islands of New Zealand encompass a complex, distributed, fault and tectonic deformation system mainly controlled by the relative motion between the Pacific and Australia plates (Fig. 1). East and north of the North Island, along the Hikurangi–Kermadec trenches, the Pacific oceanic lithosphere subducts almost orthogonally beneath the Australian plate, at a rate of 40 to 60 mm/y (1). Southward, across the South Island, oblique shear movement leads to predominant strike-slip along the Alpine fault, with a rate decreasing to ∼37 mm/y at the island's southwestern tip. Northward, subduction has created a south-narrowing volcanic arc (the Taupo volcanic chain) that extends from the tip of the Tonga–Kermadec Ridge in the Bay of Plenty across much of the North Island (e.g., ref. 2) (Fig. 2). South of the Cook Strait, subparallel, active faults slice the northern corner of the South Island, within the Marlborough area, a transitional region where the plate-boundary motion is generally interpreted to switch from subduction to strike slip (Figs. 1–3) (e.g., refs. 3 and 4).

The numerous active faults of New Zealand have produced frequent, large earthquakes in the rather short documented historical period (Fig. 2). Some of the most recent, notable events include the 1987, magnitude (M) 6.3, Edgecumbe earthquake (5); the 2010 to 2011 (moment magnitude [M_w] 7.1 and 6.2, respectively) Canterbury earthquakes (6); the 2013, M_w 6.6, Cook Strait earthquake sequence (7); and the 2016, M_w 7.8, Kaikoura earthquake (8–11). The fact that more than 20 distinct faults with variable orientations, lengths, and shear senses ruptured during the latest, 2016 Kaikoura earthquake (Fig. 3) makes it one of the most complex events ever studied (8, 9, 12–14). A better appraisal of the crustal strain and fault kinematics responsible for the 2016 event's rupture complexity is critical to elucidate the regional tectonics and assess long-term seismic hazard across the northern South Island. Such complexity implies that both remain incompletely understood.

There has been general agreement that the Marlborough fault system collectively accommodates oblique plate convergence at a rate of ∼39 mm/y, but the existence of a narrow plate boundary across that region has long been questioned (e.g., refs. 15 and 16). It was long thought that the Hope fault simply extended directly offshore to connect with the Hikurangi subduction zone (Fig. 2) (e.g., refs. 3 and 17). Recently, however, Little et al. (18) argued that localized oblique faulting within the Marlborough region extended much farther northeastward, from the Hope fault to the Jordan Thrust (JT)–Kekerengu fault, and yet farther offshore along the Needles fault (see also ref. 19).

Here, we combine observations of 1987 and 2016 coseismic slip, historical seismicity, global positioning system (GPS) measurements, and 3-dimensional slab/megathrust geometry to

Significance

The 2016, moment magnitude 7.8, Kaikoura earthquake in New Zealand's South Island generated some of the most complex surface ruptures ever observed. However, the driving mechanism for such earthquake rupture complexity remains partly unclear. By combining 2016 coseismic slip partitioning, large-scale fault kinematics, volcanism propagation, seismicity, and slab geometry, we propose that a triple junction near Kaikoura connects the 3 fastest-slipping faults of New Zealand. That triple junction kinematics accounts for the 2016 earthquake rupture complexity. Its southwest-directed migration likely drove southward stepping of strike-slip shear within the Marlborough fault system, in classic plate-tectonic fashion.

Author contributions: X.S. and P.T. designed research; X.S. and P.T. performed research; X.S., P.T., T.W., S.W., Y.W., X.W., and L.J. analyzed data; and X.S. and P.T. wrote the paper.

Reviewers: V.C., Institut De Physique Du Globe De Paris; and G.P., University of California, Los Angeles.

The authors declare no competing interest.

[1]To whom correspondence may be addressed. Email: shixuhua@zju.edu.cn or ptapponnier@gmail.com.

First published December 10, 2019.

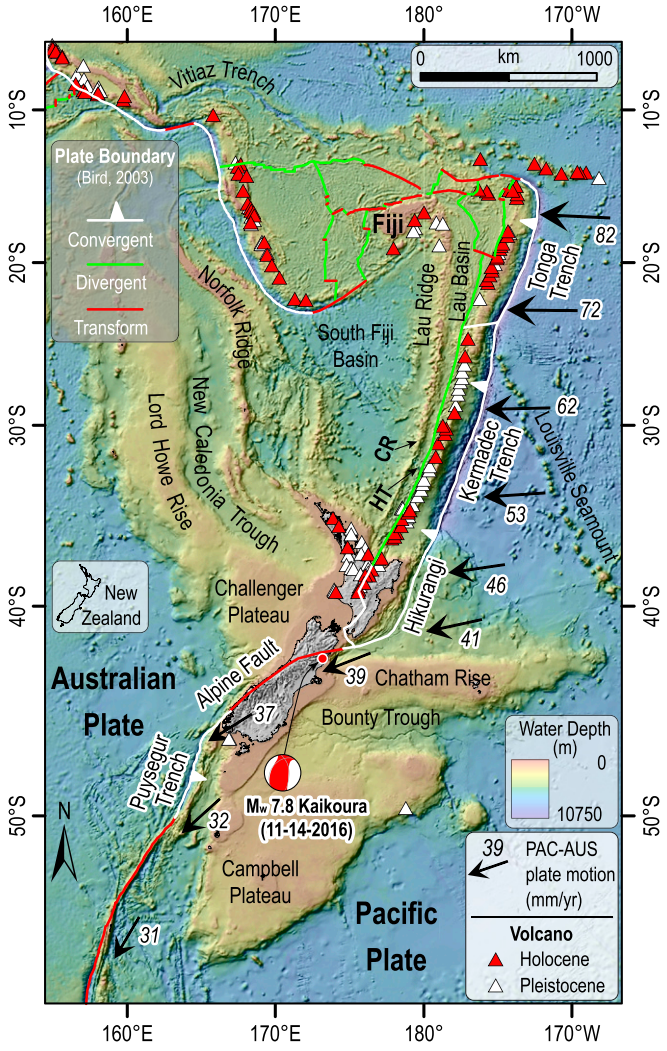

Fig. 1. Tectonic setting of the Tonga–Kermadec trench and Zealandia continent region (20), atop the ETOPO1 (1 arc-minute global relief model of Earth's surface) global relief model (85). Inferred plate and block boundaries (solid lines) are from Bird (17). The progressive, southward change of Pacific–Australia plate motion vectors is from ref. 30. Volcano locations and ages are from the Global Volcanism Program (86). CR, Colville Ridge; HT, Havre Trough.

examine the plate-boundary architecture and associated fault kinematics within and around New Zealand's South and North Islands. We suggest that the overall seismic faulting and Miocene–Holocene tectonic evolution of the region is best accounted for by the existence of a southward migrating triple junction, the "Kaikoura triple junction" (KTJ). The propagation of the 2016, M_w 7.8, Kaikoura earthquake rupture across that triple-junction area thus accounts for the exceptional intricacy of the associated coseismic faulting.

Short Summary of Neogene to Present Pacific–Australia Plate Boundary Evolution

The current plate-boundary system that crosses the New Zealand's islands is thought to have evolved from the breakup of a united Zealandia continent during Late Oligocene–Early Miocene time (~23 ± 3 million years ago [Ma]) (e.g., ref. 20). Plate reconstructions based on oceanic magnetic anomalies and finite plate rotations (e.g., refs. 4, 21, and 22) imply that subduction of the Pacific plate beneath the Australian plate along the Tonga–Kermadec and New Zealand's North Island (Hikurangi) trenches (Fig. 1) initiated at that time, although subduction in Tonga likely started earlier (23). More ancient, initial subduction north of the North Island trended northwestward, obliquely intersecting the nearly north-trending paleo-Tonga–Kermadec trench and almost perpendicular to the current NE-striking Hikurangi trench.

Recent studies (e.g., ref. 17) suggest that the obliquity of the Pacific–Australia (PAC-AUS) plate motion created the Tonga–Kermadec sliver plate. The western, oblique, boundary of this Tonga–Kermadec sliver follows the back-arc Lau basin and Havre Trough, between the Lau–Colville and Tonga–Kermadec Ridges (Fig. 1). It then continues southward within New Zealand's North Island to bisect the Taupo volcanic zone (TVZ) (Fig. 2). The eastern edge of the Tonga–Kermadec sliver plate follows the eastern PAC-AUS convergent boundary, along the Tonga–Kermadec–Hikurangi trench. The southern tip of the Tonga–Kermadec sliver is uncertain. It has been inferred to be located in the Cook Strait's submarine channel (Figs. 2 and 3) (17).

The PAC-AUS plate motion produced complex fault systems across New Zealand (Fig. 2). They include the North Island Dextral Fault Belt (or North Island Fault System [NIFS]) (24), the South Island Marlborough Fault System (MFS), and the Alpine Fault farther south, in addition to the Hikurangi megathrust and smaller offshore faults. Most of these faults are crustal scale and have been interpreted to extend down to the PAC-AUS subduction interface (e.g., refs. 25 and 26).

The NIFS includes a series of ~NNE- to north-trending dextral-slip faults in the south and multiple branches of oblique/normal faults to the north, east of the TVZ. Dextral slip on the NIFS is interpreted to have started during the Late Miocene (~7 Ma) (27) or the Early Pliocene (4 to 2 Ma) (24), possibly reactivating Early Miocene faults related to subduction along the Hikurangi margin (e.g., ref. 22). In the south, the largest faults of the NIFS are the Wellington and Wairarapa faults, with slip rates of 5 to 8 mm/y (e.g., ref. 28) and 8 to 15 mm/y (e.g., ref. 29), respectively (Fig. 3). In the southern North Island, these faults accommodate about half of the present-day ~39 mm/y PAC-AUS plate motion rate (30).

In the northern South Island, that motion is mainly accommodated by the MFS, where distributed dextral slip reportedly started around 7 Ma (31) or in the Early Pliocene (e.g., ref. 32). The MFS includes the 4, nearly parallel, NE-trending, Wairau, Awatere, Clarence, and Hope–Kekerengu dextral faults. Among them, the Hope fault to the southwest and the Kekerengu fault to the northeast have the largest slip rates, 23 ± 4 mm/y (19, 33) and 23 ± 3 mm/y (18, 34), respectively. Faulting across the MFS is thought to have migrated southeastward from the Wairau to the Hope fault since the Pliocene (e.g., ref. 31), arguably due to the southward shift of the PAC-AUS pole of rotation. Such migration kinematics has also been interpreted to account for the formation of smaller faults up to ~50 km south of the Hope fault (e.g., Porter's Pass-to-Amberley [PPA] fault zone; ref. 35). Farther to the southwest, the NE-striking Alpine fault acts as a simpler, localized, strike-slip plate boundary, with a total dextral offset of at least 450 km and possibly up to more than 700 km since ~25 Ma (e.g., ref. 36) and a Quaternary slip rate of 27.2 ± 2.4 mm/y in the north, increasing to 31.4 ± 2.8 mm/y toward the south (e.g., refs. 37 and 38).

Both the NIFS and MFS regions have experienced differential clockwise rotation since the Early Miocene, when thrust faulting started, reportedly due to the southward migration of the PAC-AUS pole of rotation. The southern NIFS and the Hikurangi margin rotated by ~3 to 4°/Ma since 20 Ma (39) and by 1 to 3°/Ma since 4 Ma (24, 39), consistent with present, geodetically derived rotation rates of 0.5 to 3.8°/Ma (40). In comparison, the MFS displays regional, differential rotations of 5 to 10°/Ma (39, 41) that occurred between 20 and 4 Ma, followed by rotations of 4 to 7°/Ma (39, 42), or locally larger (7–12°/Ma) (41), since 4 Ma. These regional and local rotations likely deflected the active fault traces in the MFS (31, 41).

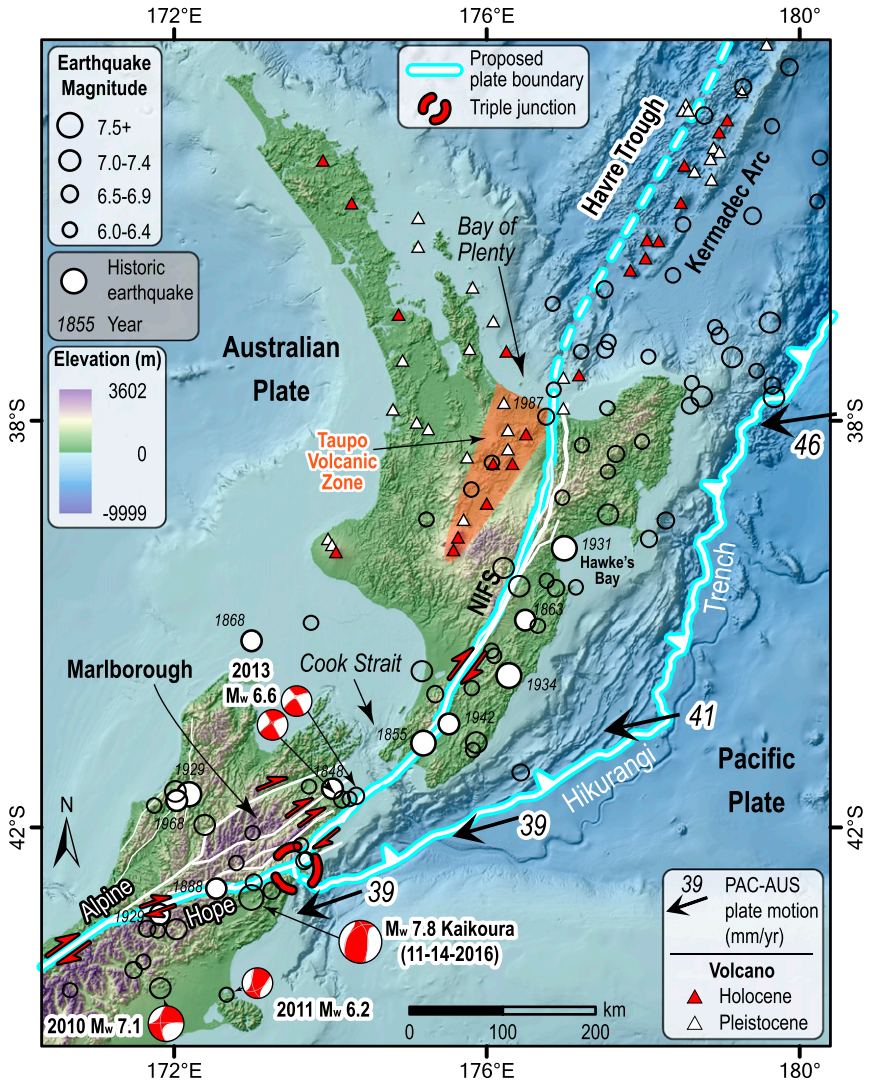

Fig. 2. Active faults, volcanoes, and seismicity of northern and central New Zealand. The light blue lines are locations of boundaries between 3 main plates (Pacific, Australian, and Tonga–Kermadec–Kaikoura sliver plate). The dashed red circle is the KTJ, as proposed in this study. Note that the KTJ is located ~150 km farther west than that inferred by Bird (17). Data sources: active faults (62, 87); 250-m-resolution bathymetry data (88); topography (89); seismicity (ref. 43 and https://earthquake.usgs.gov/earthquakes/search/); and volcanoes (86).

Since the mid-19th century, several large earthquakes with surface ruptures occurred on different faults south and north of the Cook straits (Fig. 2) (see summary in ref. 43). In the South Island, the largest ones include the 1,848, M ~ 7.5, earthquake along the Awatere fault, the 1888, M ~ 7.3, earthquake along the Hope fault (18, 33), the 1929, M ~ 7.8, Murchison earthquake, northwest of the MFS (44), and the 2016, M_w ~ 7.8, Kaikoura earthquake (8, 14). In the southeastern North Island, the largest earthquakes include the 1855, M ~ 8.2, and 1942, M ~ 7.2 Wairarapa, the 1863, M ~ 7.5, 1931, M ~ 7.3, and M ~ 7.8 Hawke's Bay, and 1934, M ~ 7.6, Pahiatua earthquakes (43, 45). The last 4 events, beneath the North Island's East coast may be related to under-thrusting along the Hikurangi Subduction zone. Other smaller earthquakes directly associated with plate-boundary faults include the 1987, M ~ 6.3 Edgecumbe earthquake, at the north end of the TVZ and NIFS (46), and the 2013, M_w ~ 6.6, Cook Strait earthquake sequence (7, 47) (Fig. 2).

Despite major, quantitative progress on regional, Miocene to present fault kinematics, how the faults link across the Cook Strait and in the MFS remains debated. In addition to the debate on the exact location of the plate boundary in the northern South Island (i.e., Alpine–Hope–Hikurangi [Fig. 2] or Alpine–Hope–Kekerengu–Needles [Fig. 3]), whether and how the MFS faults in the South Island connect with those of NIFS in the North Island through the Cook Strait (Fig. 3) remain unclear. Arguments supporting the connection of the 2 fault systems date back to the 19th century (e.g., ref. 48 and references therein), the question being how to link individual faults across the strait. Recent seismic reflection profiles show discontinuities between such faults across the Cook Strait down to a depth <3 km, which was taken to imply a disconnection between the MFS and NIFS (e.g., ref. 49). Nevertheless, based on historic evidence (50), deep seismic reflection (51) and basin stratigraphic analysis (52), the seismogenic zones along the 2 fault systems are still interpreted to be linked. Here we combine the 2016 Kaikoura earthquake coseismic slip partitioning with previous results on the PAC-AUS plate-boundary kinematics to better understand the evolution of the transitional zone between MFS, Cook Strait faulting, and NIFS.

Coseismic Slip Partitioning during the 2016 Kaikoura Earthquake

We estimate the coseismic slip partitioning in the region of the JT–Kekerengu and Papatea faults based on our published

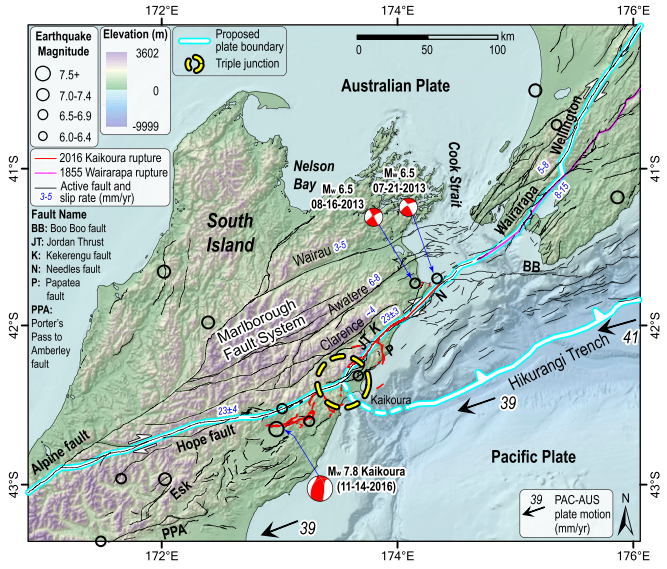

Fig. 3. Close-up view of active faults, seismicity, the KTJ, and main plate boundaries in central New Zealand. Note how the southernmost tips of sliver-plate boundaries meet to link the Hikurangi trench megathrust with the JT–Kekerengu–Needles–Wairarapa strike-slip fault. The largest horizontal seismic offsets observed in New Zealand were along the 2016 Kekerengu and 1855 Wairarapa surface ruptures. Data sources are the same as in Fig. 2.

displacement fields derived from analysis of image offsets on Sentinel-1A/B and Advanced Land Observing Satellite (ALOS)-2–based Interferometric Synthetic-Aperture Radar (InSAR) data (9) and field measurements by New Zealand's Institute of Geological and Nuclear Sciences (GNS) (e.g., refs. 12 and 14). During the 2016 earthquake, measured, dextral, surface slip along the Kekerengu fault was ∼8 to 12 m in the field (12). The Synthetic Aperture Radar-derived coseismic slip model, consistent with surface observations, yields maximum subsurface slips along and normal to the fault of ∼15 and ∼3 m, respectively (9). By comparison, the maximum dextral surface slip along the JT fault was ∼9 m (e.g., refs. 12 and 14), somewhat smaller than the maximum subsurface slip (∼11 m) (9). Dextral slip along the JT–Kekerengu fault was accompanied by nearly orthogonal, southeastward extrusion of the block south of that fault, subparallel to the Papatea fault (Fig. 4). The ratio between slip amounts parallel and normal to the average strike of the JT–Kekerengu fault is 2 to 4. Within uncertainties, this ratio is comparable to that (2.6) consistent with orthogonal partitioning of the PAC-AUS plate motion between the Hikurangi subduction and the JT–Kekerengu fault (Fig. 4 *C* and *D*). That the plate motion partitioning ratio appears to be somewhat smaller than the maximum coseismic slip ratio may indicate that part of the plate motion is also accommodated by local, vertical coseismic uplift and/or subsidence.

Nevertheless, our analysis of the coseismic slip partitioning suggests that the JT–Kekerengu fault and its offshore, northeastward extension (Needles fault) behave as a plate-boundary fault, accommodating the obliquity of PAC-AUS plate motion in the northeasternmost South Island. This inference is consistent with the fact that, based on the comparable slip rates and earthquake recurrence intervals of the Hope and Kekerengu faults (18), the plate-boundary slip along the former is predominantly transferred northeastward to the latter, and not to some offshore, unidentified extension of the Hope fault (18, 19).

The KTJ and Surrounding Plate Boundary Faulting

We propose that a plate triple junction exists southwest of the northeastern tip of the South Island. That junction, near the Kaikoura peninsula, links the 3 main and fastest slipping regional faults, namely the Hope, JT–Kekerengu–Needles, and Hikurangi megathrust. It is located about 80 km southwest of a similar junction previously inferred by Bird (17) and defines the extremity of the Kaikoura–Kermadec sliver plate (Fig. 4*B*). That there is a clear connection between the JT–Kekerengu–Needles and Wairarapa faults is a vital element of this interpretation (Figs. 3 and 4 *B* and *D*). Strong support for such a connection is the identification and very large amounts of maximum coseismic slip (15 to18 m) during the 1855, $M_w \sim 8.2$, Wairarapa earthquake (26). Like some other triple junctions, as for instance in Afar, Northeast Africa (e.g., refs. 53–55) or Iceland (e.g., ref. 56), the KTJ is not a point, but lies within a finite region. It is a fault–fault–trench (FFT)-type junction (57) between the Hope and JT strike-slip faults and the Hikurangi thrust, whose northwesternmost trace we interpret (from bathymetric morphology) to extend into the South Island margin just west of the Kaikoura peninsula, where both large south-southeastward motion and uplift were observed during the 2016 earthquake (e.g., refs. 8 and 9) (Figs. 2, 3, and 4 *A*–*D*). That interpretation is in keeping with the particularly strong (∼90°) and localized clockwise rotation of coseismic horizontal displacement vectors observed during the earthquake in that area (fig. 2 in ref. 8).

How the tip of the Kaikoura–Kermadec sliver plate crosses the Cook Strait and how the Kekerengu–Needles fault might connect with the Wairarapa fault in the North Island have not been clear (Fig. 3). Shallow seismic profiles show discontinuous, en-echelon faults in the uppermost sedimentary layers beneath the Strait (e.g., ref. 49), but deeper, more recent seismic profiles and historical earthquakes suggest that the Kekerengu and Wairarapa faults branch up from the same deep seismogenic zone (50, 51). The maximum (18.7 ± 1 m) coseismic dextral slip measured along the 1855 Wairarapa earthquake surface rupture (26) was even larger than the maximum (12 ± 0.3 m) coseismic dextral slip along the Kekerengu fault during the 2016 Kaikoura earthquake (12, 14). Such coseismic slips, that rank as the world's largest on strike-slip faults, commonly characterize great earthquakes along major transform plate boundaries (18, 58). Additionally, both events may have coruptured the subduction interface (9, 26, 59). Because the NIFS is a prominent structural feature in the North Island (e.g., ref. 24), it is thus likely that the Kermadec–Kaikoura sliver-plate western boundary extends from the Kekerengu–Needles fault across the Cook Strait to connect with the Wairarapa–North Wellington fault and its northward continuation along the NIFS to the Bay of Plenty and yet farther north (Figs. 1–3 and 5). In short, to accommodate first-order observations linked with the 2016 Kaikoura earthquake, we expand the previously inferred southwestern extremity of the Tonga–Kermadec sliver plate (Fig. 1) (17). It would extend past the southern tip of the propagating Taupo rift zone (TVZ) (Fig. 2) and across the Cook Strait, all of the way to a triple junction on the west side of the Kaikoura peninsula (Figs. 2, 3, 4*D*, and 5*A*).

Across either New Zealand or farther north along the Lau basin and Havre Trough, deformation along the western boundary of the Tonga–Kermadec–Kaikoura sliver plate coinvolves multiple active faults (60, 61). The styles and rates of such distributed deformation vary to accommodate the PAC-AUS plate motion. Overall, the contemporary regional deformation shifts from oblique, transtension in the northern North Island, to oblique, transpression in the southern North Island and northern South Island (Fig. 5). Such a spatial change is likely related to the southward increasing obliquity of PAC-AUS plate motion and has also been linked to contemporary clockwise rotation of the North Island relative to the Pacific plate (1, 39–41). In the northern North Island, transtensional, north-directed, dextral shear is accommodated by near-parallel, North-trending strike-slip fault segments that step westward across small pull-aparts (Fig. 5*B*). The cumulative rates of dextral slip and extension are estimated to be 6 to 7 mm/y (e.g., ref. 62) and 8 to 15 mm/y (e.g., ref. 63), respectively.

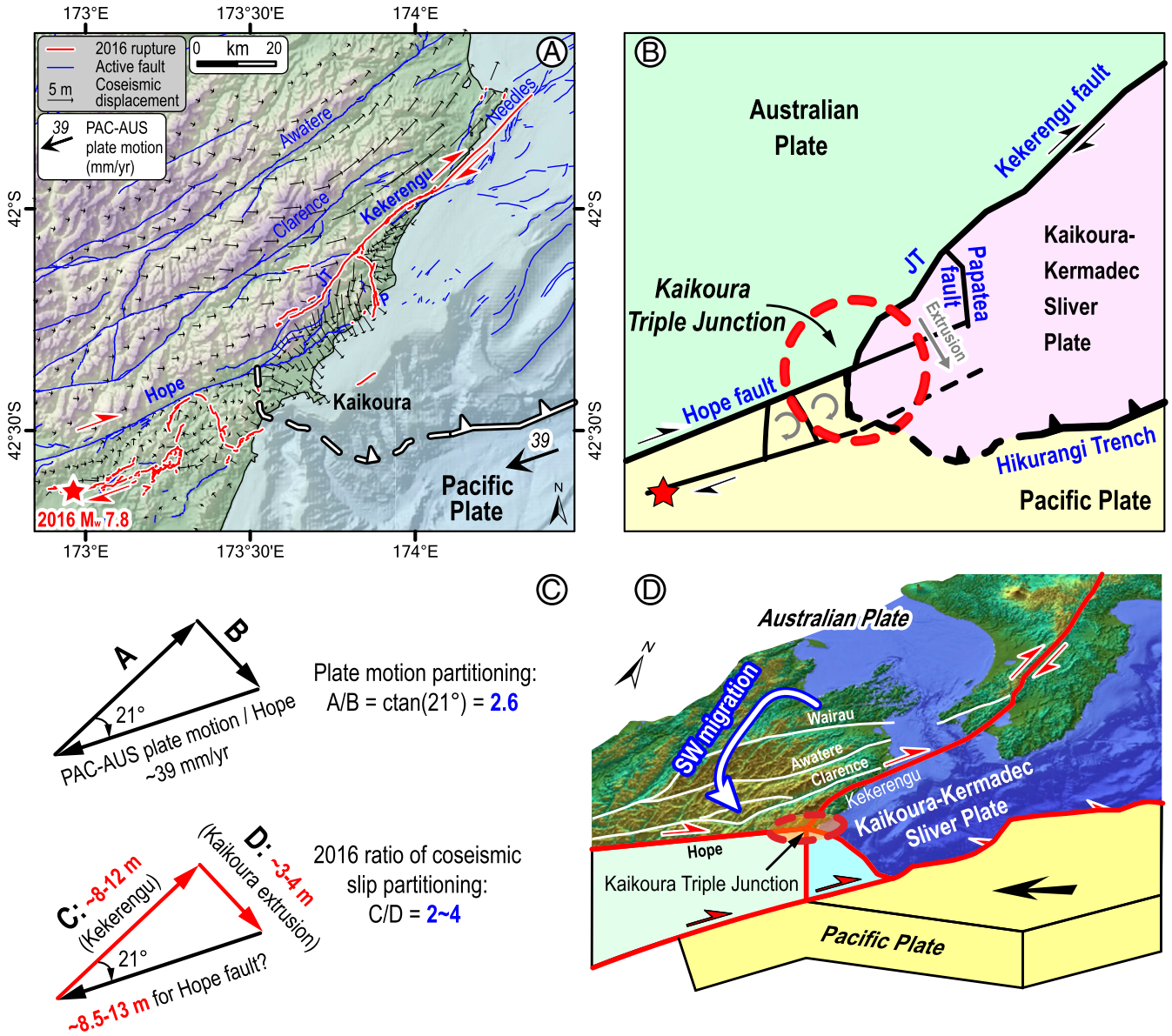

Fig. 4. Comparable 2016 coseismic slip and plate-motion partitioning support the inference that the JT–Kekerengu–Needles fault is a plate-boundary fault. (*A*) North of Kaikoura, InSAR-derived velocity vectors (9) show a sharp shift between large, nearly orthogonal coseismic movements north and south of the JT–Kekerengu fault. From Kaikoura to the 2016 epicenter, by contrast, smaller and complex motions including rotations are observed. Data sources are as in Fig. 2. (*B*) Simplified map of the KTJ showing the meeting point between nearly connected JT–Kekerengu, Hope, and Hikurangi faults at the tip of the Kaikoura–Kermadec sliver plate. The different colors identify Pacific, Australia, and Kaikoura–Kermadec plates. (*C*) Comparison between triangular vector sums of plate-motion partitioning and 2016 coseismic slip vectors on 3 main faults. (*D*) Three-dimensional block diagram view of the KTJ. Data sources are the same as in Fig. 2.

Given the obliquity of PAC-AUS plate motion at this latitude, the total convergence rate (~44 mm/y; Fig. 1) might be taken to imply ~36 mm/y of trench-normal subduction. In turn, that obliquity would thus still require as much as ~25 mm/y of NE-SW dextral shear along the NIFS. In the northern North Island and farther north offshore, along the southern Havre Trough and Kermadec volcanic arc, such dextral shear appears to be mostly accommodated by en-echelon extensional faulting, although strike-slip motion may also take place along the east side of the volcanic arc (Figs. 2 and 5*B*). Such deformation style is similar to that along the stepping pull-aparts northeast of the TVZ (Fig. 5) and was remarkably well illustrated by the superficial, en-echelon normal faulting observed during the 1987, M ~ 6.3, Edgecumbe earthquake (64, 65) (Fig. 5*B*). The extension direction consistent with that earthquake's surface rupture is identical to that fitting the regional GPS velocities (1, 40).

In the southern North Island, the partitioning of the PAC-AUS plate motion (~41 mm/y) is different because the strikes of the trench and of the Wairarapa fault are more east-westerly. This should lead to approximately equal subduction and strike-slip rates (~29 mm/y) (Fig. 2) along both the Wairarapa–Wellington faults and Hikurangi trench. Yet farther south, the present-day dextral slip along the JT–Kekerengu fault accommodates ~2/3 of the PAC-AUS plate motion (~39 mm/y) south of Kaikoura (Fig. 3). Note that the present-day GPS vector field suggests nearly complete interseismic coupling between the overriding sliver plate and the Pacific Plate (Fig. 5*A*) (66, 67), which might be taken to indicate that strain is mainly

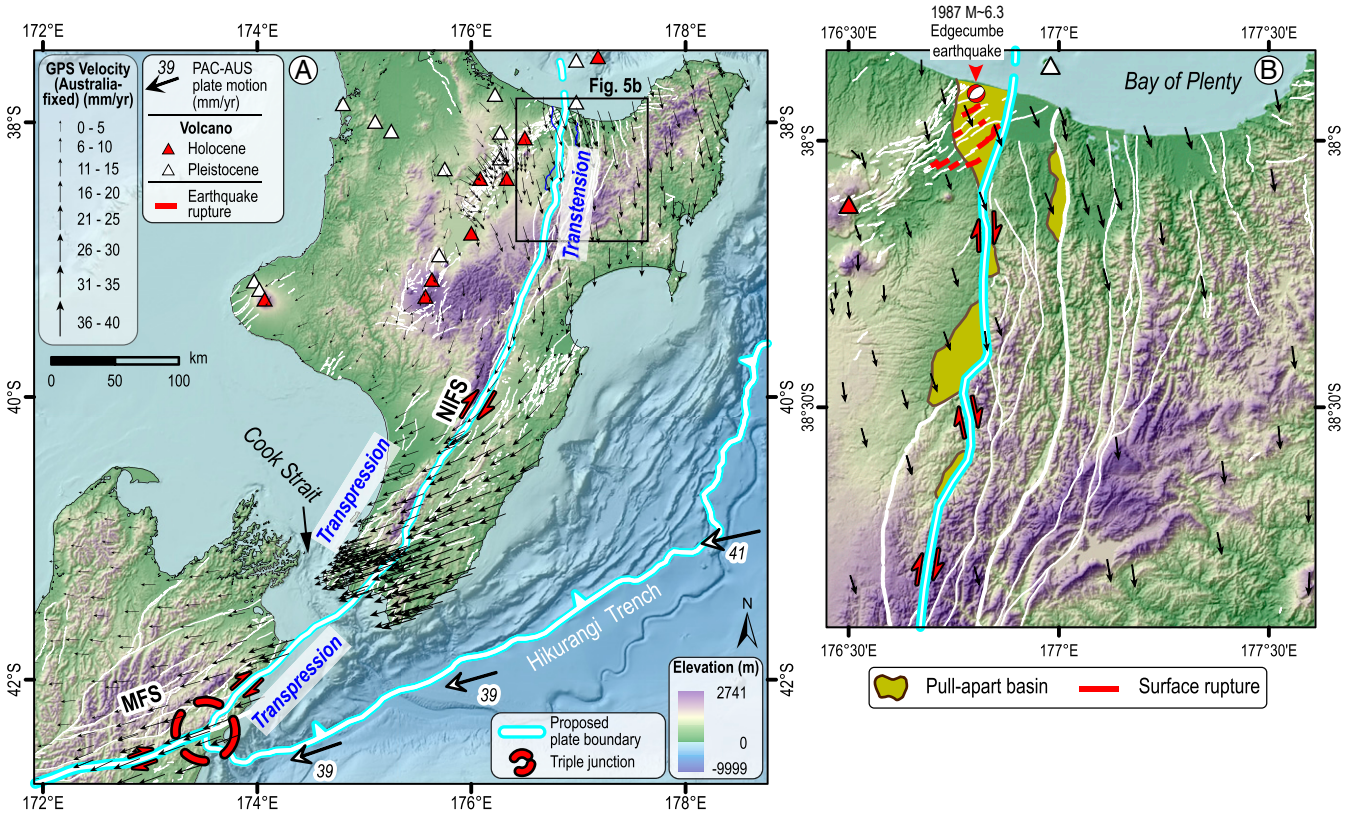

Fig. 5. Regional GPS velocity vectors relative to the Australian plate. (*A*) Variations in GPS vector orientations are consistent with a shift from regional transtension across North Island's volcanic arc to regional transpression across mountainous southern prong of that Island and South Island's Marlborough ranges (MFS). The near-orthogonal shift testifies to a sharp latitudinal stress change along the southern tip of the Tonga–Kermadec–Kaikoura sliver plate. (*B*) Close-up view of North Island's transtension volcanic/rift system. GPS vectors are nearly parallel to regional extension direction, consistent with mapped normal faulting during the 1987 Edgecumbe earthquake (red lines) (5) and with pull-apart (transparent yellow shaded) basin geometry. The GPS vector field is from ref. 1. Other data sources are as in Fig. 2.

accommodated along the western, strike-slip boundary of the Kaikoura–Kermadec sliver plate. Short-term strain variations, however, are unlikely to affect the long-term, plate-scale kinematics that we discuss in this paper.

Discussion

Inception of the Tonga–Kermadec–Kaikoura Sliver Plate and Southward Migration of the KTJ. The birthdate of the Tonga–Kermadec sliver plate has been inferred, from ages of likely contemporaneous basaltic volcanism and rifting in the Lau and Fiji basins, to be ~5 to 7 Ma (e.g., refs. 2 and 68). This may have been related to a change of Pacific plate motion during the Latest Miocene–Early Pliocene (69). At that time, the Tonga–Kermadec and the Hikurangi trenches may have met at an obtuse angle (22), or may have been aligned in a roughly northeastern direction, as they are now (21). This latest Miocene time is also that of the initiation of transpression in the Marlborough region (31). Similarly, the NIFS experienced transpression in the latest Miocene (24), a style of deformation that continues in the south, along the Wairarapa–North Wellington faults.

Volcanism in the Lau basin propagated southward to the Havre Trough (2, 70), and then to the V-shaped, SW-pointing TVZ (Fig. 1), which is reported to have formed in the last ~2 Ma (e.g., ref. 71). This observation is consistent with the southward decrease in the present-day spreading/extension rates of the Lau–Havre–Taupo system, from 120 to 145 mm/y across the Lau basin (68) to 8 to 15 mm/y across the TVZ (63). The southern tip of the Tonga–Kermadec sliver plate thus appears to have migrated southward since initiation of the Hikurangi subduction (4, 21), with a present-day, NW-trending, western limit crossing Nelson Bay in the western Cook strait (Fig. 3).

At a much larger scale, the seismicity compiled from the Advanced National Seismic System Composite Earthquake Catalog (https://earthquake.usgs.gov/earthquakes/search/) shows a clear southward decrease of the maximum focal depths of deep earthquakes, from ~700 km at ~30° south (near northern Tonga) to less than 200 km in the northern South Island at ~42° south (Fig. 6*A*). This observation is consistent with tomographic imaging along the Tonga–Kermadec PAC-AUS plate boundary that shows a southward decrease in the Pacific slab depth (Fig. 6*B*) (72). It is also consistent with the Slab2 model geometry (73). Collectively, these observations confirm a southward migration and younging of Pacific slab subduction along the Tonga–Kermadec–Hikurangi trench since its initiation during the Late Oligocene–Early Miocene (4, 22, 23).

In synch with the migration of the southern edge of the Pacific slab, the tip of the Tonga–Kermadec–Kaikoura sliver plate and the associated triple junction also migrated southwestward by ~1,000 km since the Late Miocene (7 to 5 Ma). This is attested by 3 distinct observations. First, the KTJ is an unstable FFT-type junction, as 2 of the relative velocity vectors of the 3 plates never align along a straight line (53, 57). Second, the southward migration of the sliver plate tip is reflected in the southward younging and propagation of the back-arc volcanism and rifting from the Lau basin (~7 to 5 Ma) in the northern Tonga (2), through the Havre Trough (~5 to 4 Ma) (2, 70), to the TVZ in the North Island (~2 Ma) (71). That the Taupo volcanoes evolve from relatively simple cones in the south to large calderas surrounded by far-reaching ignimbritic debris flows in the north, which

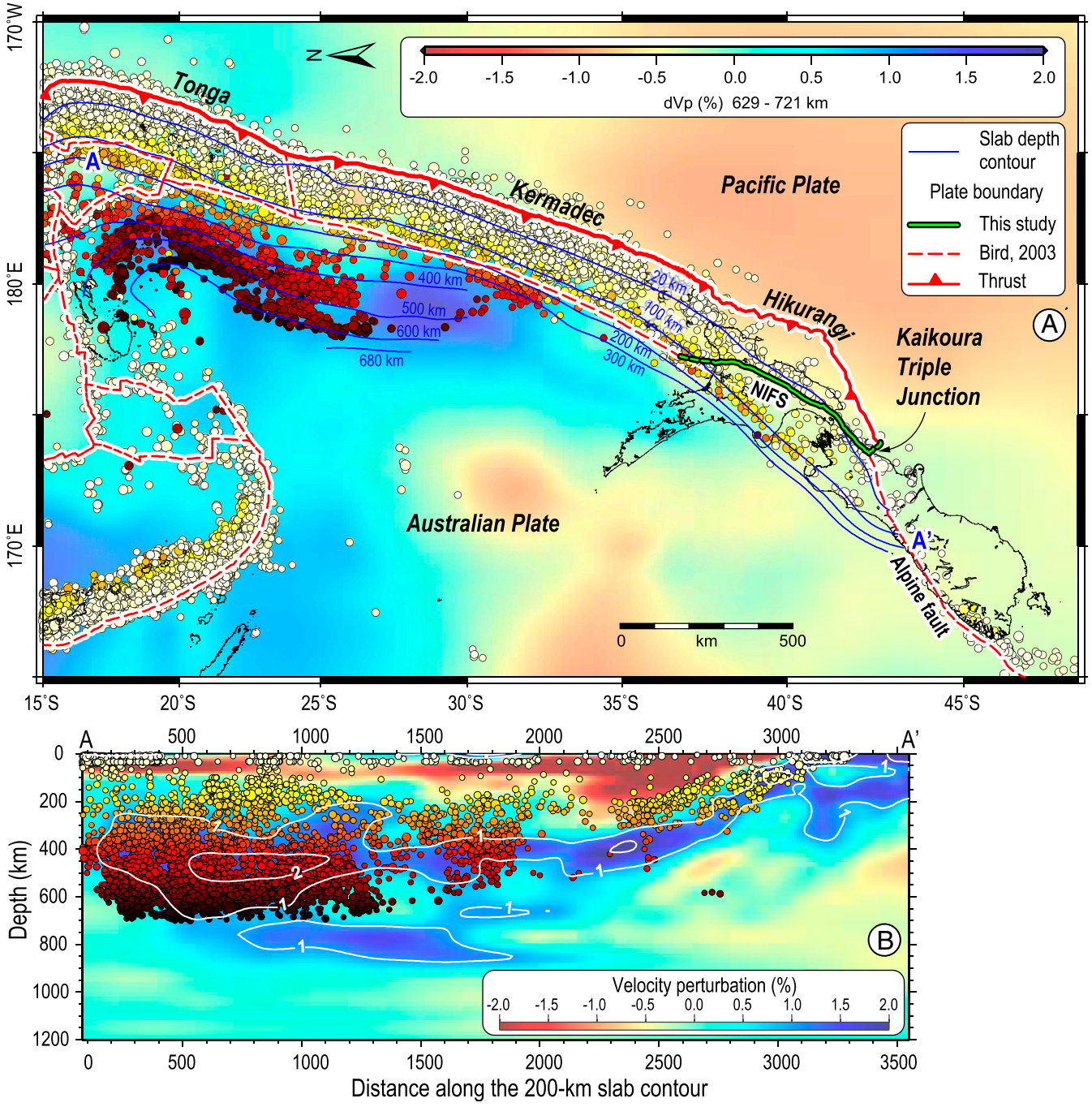

Fig. 6. Map (*A*) and A–A′ cross-section (*B*) show earthquakes' focal depths, tomographic imaging (72), and Slab2 model (73) along the Tonga–Kermadec–Kaikoura subduction zone. Both *A* and *B* suggest southward thinning of the Pacific slab (dark blue contours). Linking slab depth with subduction age implies long-term southward propagation of the KTJ.

leads to the V-shape of the volcanic zone, is also consistent, as long recognized (40, 71), with southward migration of arc volcanism (Fig. 5). Third, bathymetric data in the Lau basin (61) and the Havre Trough (60) show oblique, southeasterly extension, consistent with geodetic observations (74), and with a persistent component of right lateral slip along the sliver plate's northwest boundary.

Complex Tectonic Response to Migration of the KTJ. Tectonic deformation in regions surrounding plate-boundary system, in particular, around plate triple junctions, is often complex, with variable types of faulting, small-scale kinematic changes (e.g., refs. 55, 75, and 76), nondouble couple focal mechanisms (9, 56), surface rupture complexities (77), often coupled with volcanic and igneous activities (e.g., ref. 78). The tectonic and geomorphic response to triple-junction migration can be even more complex. For instance, the northwestward migration of California's Mendocino triple junction resulted in jumping fault systems, sedimentary basin migration and inversion, and variable changes in lithospheric structure (ref. 79 and references therein).

The migration of the KTJ into the northern South Island is probably responsible for the distributed and complex faulting

across the Marlborough System. It likely contributed to the southward shift of transform faulting from Wairau to Kaikoura (Fig. 3). The very instability of such an FFT triple junction would be consistent with successive, southwestward jumps of that junction (53, 57). Evidence supporting such southwestward shifting of faulting include: 1) the present-day geologically and geodetically derived southward increase of slip rates from the Wairau (4 ± 1 mm/y) to the Awatere (7 ± 1 mm/y) and then the Hope–Kekerengu (23 ± 3 mm/y) faults (Fig. 3) (18, 31, 33, 40); 2) the Late Holocene slip-rate decrease found along some faults in the northwestern MFS (80), particularly for the Awatere fault (81); and 3) the slip rates increase since 2 ka along portions of the Hope fault (82). It has also been proposed that fast right-lateral faulting might migrate farther to the southeast to the PPA faults (Figs. 3 and 4), newly formed faults with slip rates on the order of 3 to 4 mm/y, ~50 km south of the Hope fault (35, 40). Finally, the occurrence of ~EW, right-lateral strike-slip faulting during the 2010 to 2011 Darfield–Canterbury earthquake sequence (6), southeast of the PPA faults, may testify to incipient migration of the KTJ yet farther southeastward.

Southward shift of faulting linked with KTJ migration may partly account for the complexity of fault orientations, linkage, and interaction in the Kaikoura and Marlborough regions. The southwestward penetration of the triple junction tip into the Kaikoura upper plate may cause extreme rupture complexity in multiple directions (e.g., ref. 13). This was well illustrated by the 2016, M_w 7.8, Kaikoura earthquake deformation, that coinvolved >21 upper-plate faults of variable lengths, orientations, and shear senses, as observed geodetically and geologically (8–10, 14). Previous paleoseismic evidence has been interpreted to suggest that similar, multiple, fault-rupturing processes occurred in the past along both the Hope and Kekerengu faults (18). Also, in both the northern South Island and southern North Island, it has been argued that multiple faults ruptured simultaneously during single seismic events (50).

Complex multifault deformation and seismic ruptures in response to the KTJ migration may be associated with coseismic microblock rotations. A telltale example of this process was observed during the 2016 Kaikoura earthquake. The 2016 geodetic data revealed clear clockwise microblock rotation south of the Hope fault, with surrounding fault ruptures (Fig. 4) (9). Paleomagnetic studies (39) also show large, long-term, clockwise rotation in Neogene sedimentary rocks near the epicenter of the 2016 Kaikoura earthquake. Similar microblock rotations have long been observed near plate triple junctions, as in Afar (e.g., ref. 54), in Iceland (e.g., ref. 83), and along and near the equatorial East–Pacific rise (e.g., ref. 84). Over the long term, the KTJ migration probably contributed to regional rotation within the MFS (see above, and refs. 39–41).

Conclusion

We propose a plate-scale mechanism accounting for rupture complexity during the 2016, M_w 7.8, Kaikoura earthquake, based on links between coseismic slip partitioning and plate kinematics, fault interactions, volcanic diachronism, and deep seismicity and slab geometry along the southern extremity of the Tonga–Kermadec sliver plate in New Zealand. The complex earthquake rupture occurred along multiple faults within a triple junction area between the Pacific, Australia, and Tonga–Kermadec plates, located near Kaikoura. Within uncertainty, this mechanism is consistent with the GPS velocity fields, geological slip rates, and earthquake slip vectors across New Zealand's twin Islands. The corresponding kinematic model balances the plate-boundary velocity budget in New Zealand's South Island, accounting for the deformation amounts required to satisfy Pacific/Australia/Kermadec relative plate motions. Together with previous results on slip rates and paleoearthquakes on the Hope, Kekerengu, and Wairarapa–Wellington faults, the model implies that the JT–Kekerengu fault, Wairarapa–Wellington fault, and Hikurangi megathrust behave as the 3 major boundaries of a sliver plate, the Tonga–Kermadec–Kaikoura plate. A triple junction of FFT type thus lies near Kaikoura, which we dub the KTJ. Southwestward migration of the KTJ since the birth of the sliver plate in the Late Miocene (around 5 to 7 Ma) may have driven southward jumps of predominant strike-slip shear across the Marlborough fault system. Such temporal changes and rapid evolution account for the multiplicity of faulting, and apparently widely distributed regional strain, but the dominant slip rates (>20 mm/y) on just 3 large fault zones strongly argue for plate or block tectonics rather than diffuse lithospheric deformation within continental New Zealand.

Data Availability

All data are available in the main text or cited resources mentioned in the text.

ACKNOWLEDGMENTS. We thank New Zealand's National Institute of Water and Atmospheric Research (NIWA) for providing publicly available 250-m-resolution bathymetry; GeoNet (https://www.geonet.org.nz/) for providing seismicity catalog data; and GNS Science (New Zealand) for providing the active fault database, earthquake rupture maps and reports, and continuous GPS data. The Smithsonian Institution provided the world volcano information. We thank Christina Widiwijayanti and Lilu Cheng for collecting the volcano information. X.S. acknowledges support from Funds for International Cooperation and Exchange of the National Natural Science Foundation of China (Grant 41720104003), the AXA Research Fund, and the Hundred Talents Program of Zhejiang University (188020*194221903/011/005). P.T. acknowledges a research grant (ZDJ2019-19) from the Institute of Crustal Dynamics, China Earthquake Administration, where this work was finalized. This research was also supported by the Earth Observatory of Singapore, Nanyang Technological University, through its funding from the National Research Foundation Singapore and the Singapore Ministry of Education under the Research Centers of Excellence initiative.

1. J. Beavan *et al*., New Zealand GPS velocity field: 1995–2013. *N. Z. J. Geol. Geophys.* **59**, 5–14 (2016).
2. P. F. Ballance *et al*., Morphology and history of the Kermadec trench–arc–backarc basin–remnant arc system at 30 to 32°S: Geophysical profile, microfossil and K–Ar data. *Mar. Geol.* **159**, 35–62 (1999).
3. R. I. Walcott, Present tectonics and Late Cenozoic evolution of New Zealand. *Geophys. J. R. Astron. Soc.* **52**, 137–164 (1978).
4. K. P. Furlong, P. J. J. Kamp, The lithospheric geodynamics of plate boundary transpression in New Zealand: Initiating and emplacing subduction along the Hikurangi margin, and the tectonic evolution of the Alpine Fault system. *Tectonophysics* **474**, 449–462 (2009).
5. S. Beanland, K. R. Berryman, G. H. Blick, Geological investigations of the 1987 Edgecumbe earthquake, New Zealand. *N. Z. J. Geol. Geophys.* **32**, 73–91 (1989).
6. M. Quigley *et al*., Surface rupture during the 2010 Mw 7.1 Darfield (Canterbury) earthquake: Implications for fault rupture dynamics and seismic-hazard analysis. *Geology* **40**, 55–58 (2012).
7. I. J. Hamling *et al*., Crustal deformation and stress transfer during a propagating earthquake sequence: The 2013 Cook Strait sequence, central New Zealand. *J. Geophys. Res. Solid Earth* **119**, 6080–6092 (2014).
8. I. J. Hamling *et al*., Complex multifault rupture during the 2016 Mw 7.8 Kaikōura earthquake, New Zealand. *Science* **356**, eaam7194 (2017).
9. T. Wang *et al*., The 2016 Kaikōura earthquake: Simultaneous rupture of the subduction interface and overlying faults. *Earth Planet. Sci. Lett.* **482**, 44–51 (2018).
10. X. Shi *et al*., How complex is the 2016 Mw 7.8 Kaikoura earthquake, South Island, New Zealand? *Sci. Bull.* **62**, 309–311 (2017).
11. A. Diederichs *et al*., Unusual kinematics of the Papatea fault (2016 Kaikōura earthquake) suggest anelastic rupture. *Sci. Adv.* **5**, eaax5703 (2019).
12. J. Kearse *et al*., Onshore to offshore ground-surface and seabed rupture of the Jordan–Kekerengu–Needles fault network during the 2016 Mw 7.8 Kaikōura earthquake, New Zealand. *Bull. Seismol. Soc. Am.* **108**, 1573–1595 (2018).
13. Y. Klinger *et al*., Earthquake Damage Patterns Resolve Complex Rupture Processes. *Geophys. Res. Lett.* **45**, 10279–10287 (2018).
14. N. J. Litchfield *et al*., Surface rupture of multiple crustal faults in the 2016 Mw 7.8 Kaikōura, New Zealand, earthquake. *Bull. Seismol. Soc. Am.* **108**, 1496–1520 (2018).
15. P. Molnar *et al*., Continuous deformation versus faulting through the continental lithosphere of New Zealand. *Science* **286**, 516–519 (1999).
16. S. Bourne, P. England, B. Parsons, The motion of crustal blocks driven by flow of the lower lithosphere and implications for slip rates of continental strike-slip faults. *Nature* **391**, 655–659 (1998).
17. P. Bird, An updated digital model of plate boundaries. *Geochem. Geophys. Geosyst.* **4**, 2001GC000252 (2003).

18. T. A. Little *et al*., Kekerengu fault, New Zealand: Timing and size of Late Holocene Surface Ruptures. *Bull. Seismol. Soc. Am.* **108**, 1556–1572 (2018).
19. R. Van Dissen, R. S. Yeats, Hope fault, Jordan thrust, and uplift of the Seaward Kaikoura range, New Zealand. *Geology* **19**, 393–396 (1991).
20. B. P. Luyendyk, Hypothesis for Cretaceous rifting of east Gondwana caused by subducted slab capture. *Geology* **23**, 373–376 (1995).
21. P. J. J. Kamp, Neocene and quaternary extent and geometry of the subducted Pacific Plate beneath North Island, New Zealand: Implications for Kaikoura tectonics. *Tectonophysics* **108**, 241–266 (1984).
22. P. R. King, Tectonic reconstructions of New Zealand: 40 Ma to the present. *N. Z. J. Geol. Geophys.* **43**, 611–638 (2000).
23. S. H. A. van de Lagemaat, D. J. J. van Hinsbergen, L. M. Boschman, P. J. J. Kamp, W. Spakman, Southwest Pacific absolute plate kinematic reconstruction reveals major Cenozoic Tonga-Kermadec slab dragging. *Tectonics* **37**, 2647–2674 (2018).
24. S. Beanland, "The North Island dextral fault belt, Hikurangi Subduction Margin, New Zealand," PhD thesis, Victoria University of Wellington, Wellington, New Zealand (1995).
25. D. Eberhart-Phillips, S. Bannister, 3-D imaging of Marlborough, New Zealand, subducted plate and strike-slip fault systems. *Geophys. J. Int.* **182**, 73–96 (2010).
26. D. Rodgers, T. Little, World's largest coseismic strike-slip offset: The 1855 rupture of the Wairarapa Fault, New Zealand, and implications for displacement/length scaling of continental earthquakes. *J. Geophys. Res. Solid Earth* **111**, B12408 (2006).
27. G. Neef, Neogene development of the onland part of the forearc in northern Wairarapa, North Island, New Zealand: A synthesis. *N. Z. J. Geol. Geophys.* **42**, 113–135 (1999).
28. D. Ninis *et al*., Slip Rate on the Wellington fault, New Zealand, during the Late Quaternary: Evidence for variable slip during the Holocene. *Bull. Seismol. Soc. Am.* **103**, 559–579 (2013).
29. R. Carne, T. Little, U. Rieser, Using displaced river terraces to determine Late Quaternary slip rate for the central Wairarapa Fault at Waiohine River, New Zealand. *N. Z. J. Geol. Geophys.* **54**, 217–236 (2011).
30. C. DeMets, R. G. Gordon, D. F. Argus, S. Stein, Effect of recent revisions to the geomagnetic reversal time scale on estimates of current plate motions. *Geophys. Res. Lett.* **21**, 2191–2194 (1994).
31. T. A. Little, A. Jones, Seven million years of strike-slip and related off-fault deformation, northeastern Marlborough fault system, South Island, New Zealand. *Tectonics* **17**, 285–302 (1998).
32. G. Browne, The northeastern portion of the Clarence fault: Tectonic implications for the late Neogene evolution of Marlborough, New Zealand. *N. Z. J. Geol. Geophys.* **35**, 437–445 (1992).
33. R. Langridge *et al*., Paleoseismology and slip rate of the Conway segment of the Hope Faultat Greenburn Stream, South Island, New Zealand. *Ann. Geophys.* **46**, 1119–1139 (2003).
34. R. J. Van Dissen *et al*., "Late Quaternary dextral slip rate of the Kekerengu fault: New Zealand's third fastest on-land fault" in *GeoSciences 2016: Annual Conference of the Geoscience Society of New Zealand* (Geoscience Society of New Zealand, 2016), p. 89.
35. H. Cowan, A. Nicol, P. Tonkin, A comparison of historical and paleoseismicity in a newly formed fault zone and a mature fault zone, North Canterbury, New Zealand. *J. Geophys. Res. Solid Earth* **101** (B3), 6021–6036 (1996).
36. P. J. J. Kamp, P. G. Fitzgerald, Geologic constraints on the Cenozoic Antarctica-Australia-Pacific relative plate motion circuit. *Geology* **15**, 694–697 (1987).
37. P. M. Barnes, Postglacial (after 20 ka) dextral slip rate of the offshore Alpine fault, New Zealand. *Geology* **37**, 3–6 (2009).
38. R. Sutherland, K. Berryman, R. Norris, Quaternary slip rate and geomorphology of the Alpine fault: Implications for kinematics and seismic hazard in southwest New Zealand. *Geol. Soc. Am. Bull.* **118**, 464–474 (2006).
39. K. Randall, S. Lamb, C. M. Niocaill, Large tectonic rotations in a wide zone of Neogene distributed dextral shear, northeastern South Island, New Zealand. *Tectonophysics* **509**, 165–180 (2011).
40. L. M. Wallace, J. Beavan, R. McCaffrey, K. Berryman, P. Denys, Balancing the plate motion budget in the South Island, New Zealand using GPS, geological and seismological data. *Geophys. J. Int.* **168**, 332–352 (2007).
41. T. A. Little, A. P. Roberts, Distribution and mechanism of Neogene to present-day vertical axis rotations, Pacific-Australian plate boundary zone, South Island, New Zealand. *J. Geophys. Res. Solid Earth* **102**, 20447–20468 (1997).
42. A. P. Roberts, Tectonic rotation about the termination of a major strike-slip fault, Marlborough Fault System, New Zealand. *Geophys. Res. Lett.* **22**, 187–190 (1995).
43. GNS Science, "Where were New Zealand's largest earthquakes?" (GNS Science, 2016). https://www.gns.cri.nz/Home/Learning/Science-Topics/Earthquakes/New-Zealand-Earthquakes/Where-were-NZs-largest-earthquakes. Accessed 24 November 2016.
44. D. J. Dowrick, Damage and intensities in the magnitude 7.8 1929 Murchison, New Zealand, earthquake. *Bull. N. Z. Natl. Soc. Earthq. Eng.* **27**, 190–204 (1994).
45. GeoNet, "Geological hazard information for New Zealand" (2018). https://www.geonet.org.nz/earthquake/story. Accessed 7 July 2018.
46. I. A. Nairn, S. Beanland, Geological setting of the 1987 Edgecumbe earthquake, New Zealand. *N. Z. J. Geol. Geophys.* **32**, 1–13 (1989).
47. C. Holden, A. Kaiser, R. Van Dissen, R. Jury, Sources, ground motion and structural response characteristics in Wellington of the 2013 Cook Strait earthquakes. *Bull. New Zeal. Soc. Earthq. Eng.* **46**, 188–195 (2013).
48. G. Lensen, Note on fault correlations across Cook strait. *N. Z. J. Geol. Geophys.* **1**, 263–268 (1958).
49. N. Pondard, P. M. Barnes, Structure and paleoearthquake records of active submarine faults, Cook Strait, New Zealand: Implications for fault interactions, stress loading, and seismic hazard. *J. Geophys. Res. Solid Earth* **115**, B12320 (2010).
50. R. Grapes, G. Holdgate, Earthquake clustering and possible fault interactions across Cook Strait, New Zealand, during the 1848 and 1855 earthquakes. *N. Z. J. Geol. Geophys.* **57**, 312–330 (2014).
51. G. Holdgate, R. Grapes, Wairau basin and fault connections across Cook strait, New Zealand: Seismic and geological evidence. *Aust. J. Earth Sci.* **62**, 95–121 (2015).
52. J.-C. Audru, J. Delteil, Evidence for early Miocene wrench faulting in the Marlborough fault system, New Zealand: Structural implications. *Geodin. Acta* **11**, 233–247 (1998).
53. P. Patriat, V. Courtillot, On the stability of triple junctions and its relation to episodicity in spreading. *Tectonics* **3**, 317–332 (1984).
54. P. Tapponnier, R. Armijo, I. Manighetti, V. Courtillot, Bookshelf faulting and horizontal block rotations between overlapping rifts in southern Afar. *Geophys. Res. Lett.* **17**, 1–4 (1990).
55. I. Manighetti *et al*., Propagation of rifting along the Arabia-Somalia Plate Boundary: Into Afar. *J. Geophys. Res. Solid Earth* **103** (B3), 4947–4974 (1998).
56. G. R. Foulger, Hengill triple junction, SW Iceland 2. Anomalous earthquake focal mechanisms and implications for process within the geothermal reservoir and at accretionary plate boundaries. *J. Geophys. Res. Solid Earth* **93**, 13507–13523 (1988).
57. D. P. McKenzie, W. J. Morgan, Evolution of triple junctions. *Nature* **224**, 125 (1969).
58. R. Zinke, J. Hollingsworth, J. F. Dolan, Surface slip and off-fault deformation patterns in the 2013 MW 7.7 Balochistan, Pakistan earthquake: Implications for controls on the distribution of near-surface coseismic slip. *Geochem. Geophys. Geosyst.* **15**, 5034–5050 (2014).
59. Y. F. Bai, T. Lay, K. F. Cheung, L. L. Ye, Two regions of seafloor deformation generated the tsunami for the 13 November 2016, Kaikoura, New Zealand earthquake. *Geophys. Res. Lett.* **44**, 6597–6606 (2017).
60. J. Delteil, E. Ruellan, I. Wright, T. Matsumoto, Structure and structural development of the Havre trough (SW Pacific). *J. Geophys. Res. Solid Earth* **107**, 2143 (2002).
61. E. Ruellan, J. Delteil, I. Wright, T. Matsumoto, From rifting to active spreading in the Lau Basin–Havre Trough backarc system (SW Pacific): Locking/unlocking induced by seamount chain subduction. *Geochem. Geophys. Geosyst.* **4**, 8909 (2003).
62. N. Litchfield *et al*., A model of active faulting in New Zealand. *N. Z. J. Geol. Geophys.* **57**, 32–56 (2014).
63. I. J. Hamling, S. Hreinsdóttir, N. Fournier, The ups and downs of the TVZ: Geodetic observations of deformation around the Taupo Volcanic Zone, New Zealand. *J. Geophys. Res. Solid Earth* **120**, 4667–4679 (2015).
64. S. Beanland, G. H. Blick, D. J. Darby, Normal faulting in a back arc basin: Geological and geodetic characteristics of the 1987 Edgecumbe Earthquake, New Zealand. *J. Geophys. Res. Solid Earth* **95**, 4693–4707 (1990).
65. D. J. Dowrick, The nature and attenuation of strong ground motion in the 1987 Edgecumbe earthquake, New Zealand. *N. Z. J. Geol. Geophys.* **32**, 167–173 (1989).
66. L. M. Wallace *et al*., The kinematics of a transition from subduction to strike-slip: An example from the central New Zealand plate boundary. *J. Geophys. Res.* **117**, B02405 (2012).
67. L. M. Wallace *et al*., Triggered slow slip and afterslip on the southern Hikurangi subduction zone following the Kaikōura earthquake. *Geophys. Res. Lett.* **45**, 4710–4718 (2018).
68. J. W. Hawkins, "The Geology of the Lau Basin" in *Backarc Basins: Tectonics and Magmatism*, B. Taylor, Ed. (Springer, Boston, MA, 1995), pp. 63–138.
69. J. Austermann *et al*., Quantifying the forces needed for the rapid change of Pacific plate motion at 6Ma. *Earth Planet. Sci. Lett.* **307**, 289–297 (2011).
70. L. M. Parson, I. C. Wright, The Lau-Havre-Taupo back-arc basin: A southward-propagating, multi-stage evolution from rifting to spreading. *Tectonophysics* **263**, 1–22 (1996).
71. C. J. N. Wilson *et al*., Volcanic and structural evolution of Taupo volcanic zone, New Zealand: A review. *J. Volcanol. Geotherm. Res.* **68**, 1–28 (1995).
72. Y. Fukao, M. Obayashi, Subducted slabs stagnant above, penetrating through, and trapped below the 660 km discontinuity. *J. Geophys. Res. Solid Earth* **118**, 5920–5938 (2013).
73. G. P. Hayes *et al*., Slab2, a comprehensive subduction zone geometry model. *Science* **362**, 58–61 (2018).
74. M. Bevis *et al*., Geodetic observations of very rapid convergence and back-arc extension at the Tonga arc. *Nature* **374**, 249 (1995).
75. C. Doubre *et al*., Current deformation in Central Afar and triple junction kinematics deduced from GPS and InSAR measurements. *Geophys. J. Int.* **208**, 936–953 (2017).
76. G. Peltzer, F. Crampé, S. Hensley, P. Rosen, Transient strain accumulation and fault interaction in the Eastern California shear zone. *Geology* **29**, 975–978 (2001).
77. E. Jacques *et al*., Normal faulting during the August 1989 earthquakes in central Afar: Sequential triggering and propagation of rupture along the Dobi Graben. *Bull. Seismol. Soc. Am.* **101**, 994–1023 (2011).
78. R. S. Marshak, D. E. Karig, Triple junctions as a cause for anomalously near-trench igneous activity between the trench and volcanic arc. *Geology* **5**, 233–236 (1977).
79. K. P. Furlong, S. Y. Schwartz, Influence of the Mendocino triple junction on the tectonics of coastal California. *Annu. Rev. Earth Planet. Sci.* **32**, 403–433 (2004).
80. P. L. Knuepfer, Temporal variations in latest Quaternary slip across the Australian-Pacific plate boundary, northeastern South Island, New Zealand. *Tectonics* **11**, 449–464 (1992).
81. T. A. Little, R. Grapes, G. W. Berger, Late Quaternary strike slip on the eastern part of the Awatere fault, South Island, New Zealand. *Geol. Soc. Am. Bull.* **110**, 127–148 (1998).
82. N. Khajavi, A. Nicol, M. C. Quigley, R. M. Langridge, Temporal slip-rate stability and variations on the Hope Fault, New Zealand, during the late Quaternary. *Tectonophysics* **738-739**, 112–123 (2018).
83. A. J. Horst, J. A. Karson, R. J. Varga, Large rotations of crustal blocks in the Tjörnes Fracture Zone of Northern Iceland. *Tectonics* **37**, 1607–1625 (2018).
84. R. N. Hey *et al*., Microplate tectonics along a superfast seafloor spreading system near Easter Island. *Nature* **317**, 320–325 (1985).
85. C. Amante, "ETOPO1 1 arc-minute global relief model: Procedures, data sources and analysis" (NOAA Technical Memorandum NESDIS NGDC-24, National Geophysical Data Center, National Oceanic and Atmospheric Administration, 2009). https://www.ngdc.noaa.gov/mgg/global/. Accessed 7 July 2018.
86. Smithsonian Institution, Global Volcanism Program (2018). https://volcano.si.edu/. Accessed 30 July 2018.
87. R. Langridge *et al*., The New Zealand active faults database. *N. Z. J. Geol. Geophys.* **59**, 86–96 (2016).
88. J. S. Mitchell *et al*., Undersea New Zealand, 1: 5,000,000 (National Institute of Water and Atmospheric Research Chart, Miscellaneous Series No. 92, 2012).
89. T. G. Farr *et al*., The Shuttle radar topography Mission. *Rev. Geophys.* **45**, RG2004 (2007).